Synthesis and Structure Determination of Ytterbium Nanoparticles

Jorge A. Ascencio,*[†,††] Ana C. Rodríguez-Monroy,[††] Hong Bo Liu,[†] and Gerardo Canizal[†]
[†]*Instituto Mexicano del Petroleo, Lázaro Cárdenas No. 152,*
Col. San Bartolo Atepehuacan, C.P.07730, Mexico D. F., Mexico
[††]*Facultad de Quimica, Universidad Autonoma del Estado de Mexico,*
Paseo Colon esq. Paseo Tollocan, Toluca, Mexico. C. P. 50120, Mexico

(Received April 15, 2004; CL-040419)

For the first time the synthesis of of Yb metal nanoparticles is reported. The synthesis was made using the bioreduction methods. By the change in the pH the nanoparticles of 2 up to 10 nm were obtained. Size and structure determination was made using low magnification and high resolution transmission electron microscopy, which demonstrated that the particles are mainly of fcc-like structures. Theoretical calculations for by of molecular dynamics simulation for configurations with 4000 atoms of the Yb nanoparticle demonstrated that the fcc-like structure is the lowest energy configuration.

An important goal of nanotechnology is to develop new materials at the nanometric scale, because their properties change dramatically as a function of the size and local structure. This behavior has opened the field of nanomaterials in applications of catalysis,[1] optoelectronics,[2] and medicine.[3] One of the objectives of research is to obtain nanoparticles with specific characteristics.

Recently the reduction of lanthanide salts to nanoparticles has been reported for Eu with Au[4] with perspectives of application in photonic devices and for samarium focused to nuclear medicine uses. These rare earth elements have important peculiarities because their big number of electrons and their possibility to be radioactive. Ytterbium is a particularly interesting element because of its capacity to vary its valence under different conditions. After its discovery by Marignac in 1878, the preparation in metallic form was achieved by Klemm and Bommer in 1937;[5] Yb has been applied in optical devices. Yb has ^{169}Yb radioisotope, which is used for portable industrial unities with high intensity radiographs.

One synthesis method that has proved to be able of producing lanthanide nanoparticles is the bioreduction method, which is based in the use of biomass for reducing metal nanoparticles.[4,6] It has been used for Au nanoparticles[6] and bimetallic nanoparticles.[4] The main parameter to control the nanoparticles formation is the pH used during the synthesis, as reviewed in previous reports. In this work, we report the use of bioreduction method controlling the pH at 4, 6, 7, and 8, in order to determine the optimum conditions for the smallest nanoparticles and the higher quantity of clusters. Transmission electron microscopy (TEM) by a JEOL 2010 energy dispersive spectroscope (EDS) and high resolution (HRTEM) by a JEOL 4000EX microscope were employed to characterize the size distribution, composition, and internal structure of the samples.

It was concluded that at pH = 4 no nanoparticles were genenated, because Yb was not identified in local areas, and the TEM contrast denoted just the biomass aggregation. However, at the other pH values, the Yb nanoparticles were evident. In order to determine the size distribution, low magnification images were used to analyze the samples, obtaining well-defined modes at each pH as it can be observed in Figure 1. In the figure, it displays the image of samples prepared at a) pH = 6, b) pH = 7, and c) pH = 8 images; besides the size distribution plot (Figure 1d) and a common EDS spectra from the samples. It is clear that the of nanoparticle size distribution is different at each pH condition: high dispersed for pH = 6 around 4 nm, lower dispersed with the maximum around 2 nm for pH = 7 and bigger than 7 nm for almost all particles for pH = 8.

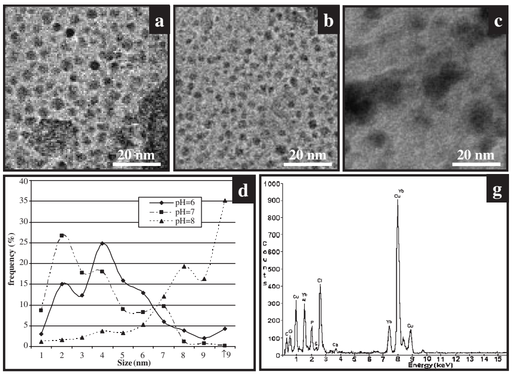

Figure 1. TEM micrographs for samples synthesized at a) pH = 6, b) pH = 7, and c) pH = 8, with d) the corresponding size distribution plot for them, and e) a common EDS spectra for the samples.

The elemental distribution observed in the EDS spectra denotes the existence of Yb and the biomass-identified elements (C, O, P, S, Cl, and Ca) besides Cu from the grid. Therefore, the aggregation structure must be studied in more detail, and we used HRTEM to determine the internal structure. In the Figure 2, HRTEM images for the different samples are shown with their corresponding fast Fourier transforms for identifying their frequencies from the observed structures. Figures 2a and 2b are images of particles produced at pH = 6; the first one corresponds to a nanoparticle of 4.6 nm with hexagonal contrast in the center and parallel lines around the cluster; also its corresponding FFT shows the hexagon besides extra dots that are produced by the materials around it. The image in Figure 2b shows an fcc-like nanoparticle of 4.2 nm in the {011} orientation,[7] with well-defined faces and a hexagonal symmetry in the FFT. The measured interplanar distances match with Yb bulk,[8] which are of 3.16 and 2.74 Å in the direction of [111] and [200], respectively. Nanoparticles obtained at pH = 7 are shown in Figures 2c and 2d. Figure 2c shows a cluster of 4.2 nm with contrast lines common for fcc-like clusters in the [013] orientation.[7] Besides, several small particles ($\approx$1.8 nm) are observed in Figure 2d, and in the center a well-defined hexagonal shape with similar internal structure can be seen as it is confirmed by the FFT; it is important to notice the small defects in the image (note the different distances in left and right marks) and in the FFT, which must be produced by the surface constrain as it has been demonstrated for nanoparticles passivated by thiols.[9] Finally a couple of images of samples prepared at pH = 8 are shown in Figures 2e and 2f; big clusters can be observed and they present also effects in the contrast common for wide crystals including the second order frequencies in the internal zone of the FFT. While the image in Figure 2f shows local domains of different contrast with zones of well-defined dots and small deformations, which are associated to the thickness and the orientation near the [001] direction. In both cases the structures are bigger than 10 nm and the interplanar measured distances match with the bulk data.

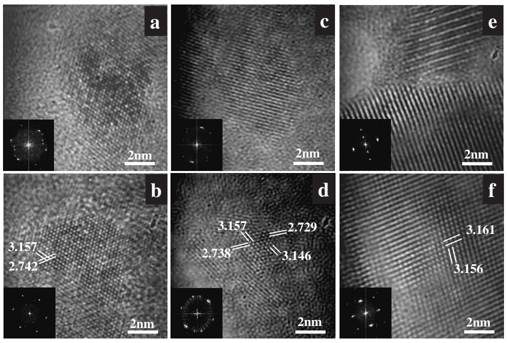

Figure 2. HREM images of samples at pH 6 (a,b), pH 7 (c,d) and pH 8 (e,f) with their FFT and inter-planar distance measurements.

In order to support the observed structures and to understand the stability of the particles we applied molecular dynamics simulations to clusters up to 4000 atoms. An EAM for ytterbium was constructed by Bhuiyan et al.[10] on the basis of the original work of Daw and Baskes,[11] where the embedding energy is cubic spline interpolation function. Spline knots and the other potential parameters in pair potential and electronic density are fitted to the physical properties such as average bulk and shear moduli and the sublimation energy of solid. In this work, within the frame of Bhuiyan, the EAM for ytterbium was improved by the introduction of Rose relationship for solid.[12] Particularly, the pair potential and the electron density take the same forms and parameters as Bhuiyan's model[9] but the embedding energy was produced by Rose relationship. The used models correspond to the lowest energies geometries for the most of metals based in fcc-like (truncated octahedron) and multiple twin particles (decahedron and icosahedron).[13] Figure 3 shows the plot of cohesive energy per atom for the truncated octahedral (TO), decahedral (Dh), and icosahedral (Ih). It is clear how the TO structures are more stable than the multiple twin particles in all the cases. This effect is observed in other metals in big clusters, where the bulk behavior domains the structure.[14]

For Yb this effect must be more important because of the size of the atoms, implying higher strain for smallest nanoparticles, but for the range that we obtained, the tendency to the bulk structure is dominant.

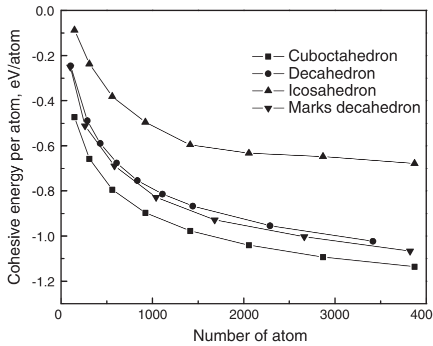

Figure 3. Plot of cohesive energy per atom vs. number of atoms for the 4 types of main metal cluster configurations.

The possibility of generating Yb nanoparticles extends the field of applications of nanotechnology, because of the actual importance of Yb in optical and other fields and the perspectives of manipulating its properties in the nanometric range. Besides, the control of particle size by an easy, cheap method allows synthesizing clusters with important properties based on its size and composition. In this work, we reported the synthesis of nanoparticles of hundreds to thousand of atoms by bioreduction method and with just one configuration type, fcc-based structure. The HREM showed that the particles are of this kind, and for the smallest particles there are evidence of lattice deformations, which imply the surface energy reduction. This work opens a new perspective in the use of Yb and rare earth pure clusters with their unique properties as candidates for band gap manipulation, and even radio-pharmaceutical uses in the near future by means of the structure control and improved synthesis.

References

1 C. T. Campbell, S. C. Parker, and D. E. Starr, *Science*, **298**, 811 (2002).
2 Z. Tang, N. A. Kotov, and M. Giersig, *Science*, **297**, 237 (2002).
3 D. F. Emerich and C. G. Thanos, *Expert Opin. Biol. Ther.*, **3**, 655 (2003).
4 J. A. Ascencio, Y. Mejia, H. B. Liu, C. Angeles, and G. Canizal, *Langmuir*, **19**, 5882 (2003).
5 G. Hampel, "The Encyclopedia of Chemical Elements," Reinhold Book Corporation, U.S.A. (1992).
6 J. Gardea-Torresday, K. Tiemman, G. Gamez, K. Dokken, S. Tehuacanero, and M. Jose-Yacaman, *J. Nanopart. Res.*, **1999**, 1.
7 J. A. Ascencio, C. Gutiérrez-Wing, M. E. Espinosa-Pesqueira, M. Marín, S. Tehuacanero, C. Zorrilla, and M. José-Yacamán, *Surf. Sci.*, **396**, 349 (1998).
8 G. Klem and N. Z. Bommer, *Inorg. Chem.*, **231**, 152 (1937).
9 M. José-Yacamán, S. Tehuacanero, C. Zorrilla, J. A. Ascencio, and A. Gómez, *Nanostruct. Mater.*, **10**, 1 (1998).
10 G. M. Bhuiyan and M. A. Khaleque, *J. Non-Cryst. Solids*, **226**, 175 (1998); G. M. Bhuiyan, M. Sibert, and M. J. Stott, *Phys. Rev. B*, **53**, 636 (1996).
11 S. Daw and M. I. Baskes, *Phys. Rev. B*, **29**, 6443 (1984).
12 J. H. Rose, J. R. Smith, F. Guinea, and J. Ferrante, *Phys. Rev. B*, **29**, 2963 (1984).
13 H. B. Liu, J. A. Ascencio, M. Perez-alvarez, and M. J. Yacaman, *Surf. Sci.*, **491**, 88 (2001).
14 M. José-Yacamán, J. A. Ascencio, and H. Liu, *J. Vac. Sci. Technol., B*, **19**, 1091 (2001).

Published on the web (Advance View) July 24, 2004; DOI 10.1246/cl.2004.1056